

Optically Pumped Polarized ${}^3\text{He}^{++}$ Ion Source Development for RHIC/EIC

A. Zelenski^a, G. Atoian^a, E. Beebe^a, S. Ikeda^a, T. Kaneshue^a, S. Kondrashev^a, J. Maxwell^{b,c}, R. Milner^b, M. Musgrave^b,
M. Okamura^a, A. A. Poblaguev^{a,*}, D. Raparia^a, J. Ritter^a, A. Sukhanov^a, S. Trabocchi^a

^aBrookhaven National Laboratory, Upton, NY 11973, USA

^bLaboratory for Nuclear Science, Massachusetts Institute of Technology, Cambridge, MA 02139, USA

^cThomas Jefferson National Accelerator Facility, Newport News, VA 23606, USA

Abstract

The proposed polarized ${}^3\text{He}^{++}$ acceleration in RHIC and the future Electron-Ion Collider will require about 2×10^{11} ions in the source pulse. A new technique had been proposed for production of high intensity polarized ${}^3\text{He}^{++}$ ion beams. It is based on ionization and accumulation of the ${}^3\text{He}$ gas (polarized by metastability-exchange optical pumping and in the 5 T high magnetic field) in the existing Electron Beam Ion Source (EBIS). A novel ${}^3\text{He}$ cryogenic purification and storage technique was developed to provide the required gas purity. An original gas refill and polarized ${}^3\text{He}$ gas injection to the EBIS long drift tubes, (which serves as the storage cell) were developed to ensure polarization preservation. An infrared laser system for optical pumping and polarization measurements in the high 3–5 T field has been developed. The ${}^3\text{He}$ polarization 80–85% (and sufficiently long ~ 30 min relaxation time) was obtained in the “open” cell configuration with refilling valve tube inlet and isolation valve closed. The development of the spin-rotator and ${}^3\text{He}^4\text{He}$ absolute nuclear polarimeter at 6 MeV ${}^3\text{He}^{++}$ beam energy is also presented.

Keywords: Polarization, Optical pumping, EBIS (Electron Beam Ion Source).

1. Introduction

The Relativistic Heavy Ion Collider [1] (RHIC) at Brookhaven National Laboratory (BNL) is the first high-energy accelerator-collider complex where the *Siberian Snake* technique [2] has been successfully implemented to avoid the resonance depolarization during the beam acceleration and yields 60% polarization for colliding beams. It also serves as the home for the future Electron-Ion Collider [3] (EIC). The ${}^3\text{He}^{++}$ polarization can be preserved during acceleration in high-energy synchrotron accelerators like the Alternating Gradient Synchrotron and RHIC by using the *Siberian snake* technique. The nuclear polarization in a polarized ${}^3\text{He}^{++}$ beam is carried mostly by neutrons. Therefore, high-energy collisions of polarized electrons and neutrons can be effectively studied at EIC with the polarized ${}^3\text{He}^{++}$ beam.

The proposed polarized ${}^3\text{He}^{++}$ acceleration in RHIC will require about 2×10^{11} ions in the source pulse and about 10^{11} ions in the RHIC bunch. To deliver this intensity in a $20 \mu\text{s}$ pulse duration for the injection to the Booster, the source peak current has to be about $2000 \mu\text{A}$, which is $\times 1000$ higher than ever achieved in previous ${}^3\text{He}^{++}$ ion sources. We have proposed the concept for a polarized ${}^3\text{He}^{++}$ ion source based on the existing Electron Beam Ion Source (EBIS) at BNL [4, 5, 6]. The ${}^3\text{He}$ atoms are polarized via the Metastability Exchange Optical Pumping technique [7, 8] in a glass cell at a pressure of 1–10 mbar in a high-field 5.0 T magnetic field within the EBIS

solenoid and then will be injected into the EBIS ionizer. The ionization is produced in the 5.0 T magnetic field. This field is much higher than the critical 0.31 T field for ${}^3\text{He}^+$ ions, therefore the depolarization in the intermediate single-charged ${}^3\text{He}^+$ states is strongly suppressed (to less than 1%). Some polarization losses may occur during ionization in the low field near solenoid edges. These effects will be studied experimentally with the polarized ${}^3\text{He}^{++}$ beam. The simulations show that polarization losses should not exceed a few (3–5) percent and the nuclear polarization of the ${}^3\text{He}^{++}$ beam in excess of 70% can be achieved in this source.

In the EBIS, an estimated $(2.5\text{--}5.0) \times 10^{11}$ ${}^3\text{He}^{++}$ ions can be produced and accumulated in the long 1.5 m EBIS trap region. The total charge capacity is estimated at about 10^{12} based on the total electron beam charge and a neutralization factor of about 0.5. The required beam intensity of 2×10^{11} ${}^3\text{He}^{++}$ /pulse can then be obtained during extraction and acceleration in a single beam pulse.

Successful tests of polarizing ${}^3\text{He}$ in a high magnetic field [9, 10, 11, 12] have led to the development of the Extended EBIS concept. This upgrade will also improve the heavy ion and gas species production. The Extended EBIS upgrade is now an approved Accelerator Improvement Project at BNL with the primary purpose of increasing the Au^{32+} intensity, but it will provide essential infrastructure for the polarized ${}^3\text{He}$ ion source.

2. Polarized ${}^3\text{He}^{++}$ Ion Source

The EBIS currently produces high charge state ions for injection to RHIC and will remain the primary source of charged

*Corresponding author

Email address: poblaguev@bnl.gov (A. A. Poblaguev)

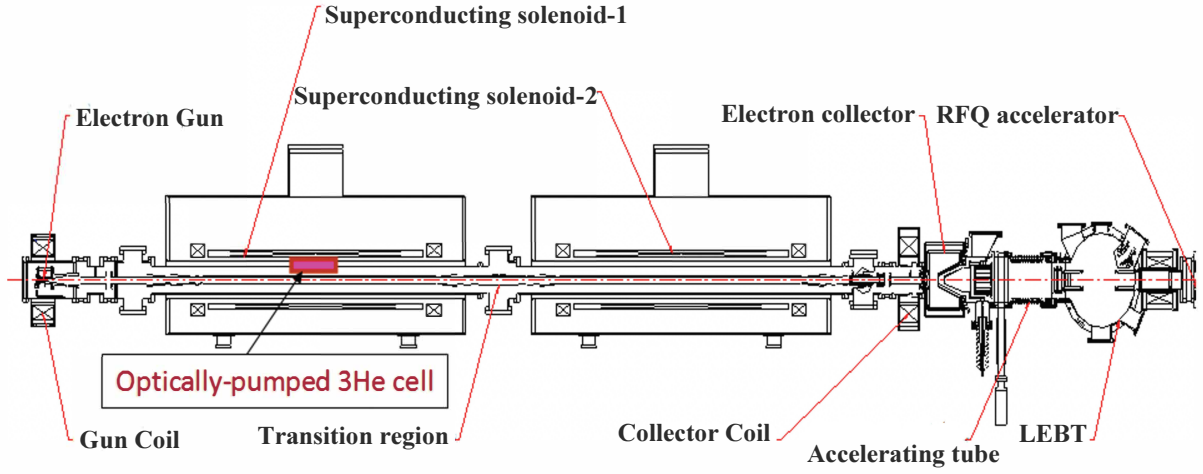


Figure 1: Schematic diagram of the extended EBIS. The polarized ^3He gas is injected into the drift tube of the new “injector” EBIS section. Here, RFQ means Radio Frequency Quadrupole and LEBT is the Low Energy Beam Transport.

ions from protons to Uranium for the future EIC. In the EBIS, the high intensity (10 A) electron beam is produced by the electron gun with cathode diameter 9.2 mm and injected into the 5.0 T solenoid magnetic field. The electron beam is radially compressed by the magnetic field to a diameter of about 1.5 mm in the ionization region and then expanded before dumping into the electron collector at the other end. Ions are radially confined by the space charge of the electron beam and longitudinally trapped by electrostatic barriers at the ends of the trap region. The ions are extracted by raising the potential of the trap and lowering the barrier [13]. A second 5.0 T solenoid has been constructed as an element in the extended EBIS upgrade. The polarized ^3He gas will be injected and ionized in the upstream solenoid, and $^3\text{He}^+$ ions will be trapped and further ionized to the $^3\text{He}^{++}$ state in the downstream solenoid (see Fig. 1).

The ^3He gaseous cell will be placed inside the EBIS “injector” solenoid and the pulsed gas valve (similar to the valve in the BNL Optically Pumped Polarized Ion Source [14]) will be used for the gas injection into the center of the EBIS drift tube system to minimize depolarization and increase ionization efficiency. The second “injector” EBIS section allows the use of differential pumping between the “gas injector” and the main EBIS. This is especially beneficial for gas species production (including ^3He gas). An isolation valve between the two EBIS sections will simplify the ^3He polarizing apparatus maintenance. The ionization in the EBIS is produced in a 5.0 T magnetic field, which preserves the nuclear ^3He polarization while in the intermediate single-charged $^3\text{He}^+$ state. The number of ions is limited to the maximum charge, which can be confined in the EBIS. From experiments with Au^{32+} ion production, one expects more than 2×10^{11} $^3\text{He}^{++}$ ions/pulse to be produced and extracted for the subsequent acceleration and the injection into RHIC. After the $^3\text{He}^{++}$ beam acceleration to the energy 6 MeV the absolute nuclear polarimeter based $^3\text{He}^4\text{He}$ collisions will be used for the polarization measurements.

The high ^3He nuclear polarization in excess of 80% was achieved by the metastability-exchange technique in the sealed glass cell in the high 2.0–4.0 T magnetic field. In these measurements, the ^3He gas at 1.0–3.0 Torr pressure was contained in the glass cell and the weak RF discharge was introduced to populate the metastable states. Metastable atoms in the 2^3S_1 state were polarized by optical pumping with circularly polarized ($2^3\text{S}_1 - 2^3\text{P}_0$) 1083 nm laser light. Any contamination in the helium gas cell (hydrogen, water vapor etc.) reduces the ^3He polarization due to metastable states quenching.

3. ^3He Gas Purification and Cell Filling System

The gas purity in the sealed cell was achieved by use of an elaborate glass cell cleaning, baking, outgassing procedure and sophisticated gas purification system. In the polarized source, the optically pumped cell must be connected to the valve for gas injection to the drift tube and the line for the gas refill. To eliminate contamination and to maintain the necessary gas purity in this “open cell” configuration we developed the system for ^3He gas purification and filling based on the technique of cryo-pumping, which pumps all gases except for the helium. In a conventional two stage cryopump we cut away half of the cryo-panel (the second part is required to maintain the isolation vacuum) and installed the additional cold vessel (attached to the cold head of the cryo-pump) filled with charcoal granules (see Fig. 2).

It was connected to the ^3He filling system by a thin vacuum bellows (see Fig. 2). At the operational temperatures of 20–25 K, the pump was continuously absorbing (and reducing the partial pressures of hydrogen, water, hydrocarbons, and argon) to the level below 10^{-7} Torr. This pump absorbs also quite a significant amount of ^3He gas (about 100 cm^3). The absorbed gas is released by the vessel heating with a built-in cartridge

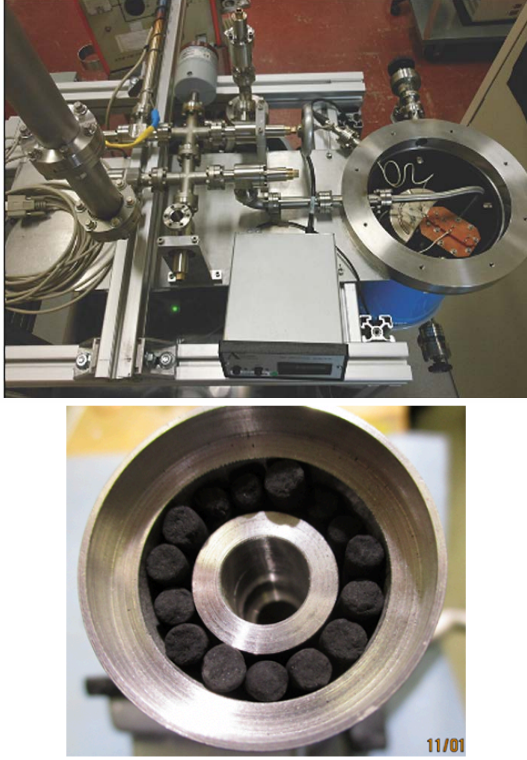


Figure 2: Top: the cryogenic ^3He purification and filling system. Bottom: the vessel filled with charcoal granules is attached to the cold head of the cryo-pump.

heater. This provides gas storage and supply for ^3He -cell operation at the optimal optical-pumping pressure of 3–5 Torr. The pressure stability is maintained with the heater feedback system on the gas pressure measured by a Baratron MKS-626 pressure transducer.

The optically pumped ^3He glass cell is attached to the gas filling system with a 200 cm long stainless tube. The cell and filling system were mounted on a movable support and inserted inside the superconducting solenoid. To prevent ^3He atoms depolarization due to travel through the solenoid gradient field we installed an additional isolation valve close to the cell in the homogeneous field region. Initially we used copper tube coupling and a commercial pneumatic-driven valve, which produced quite a bit of contamination and diffusion in the tube outside of the cell. As the latest improvement, we developed a new remotely controlled (pneumatic) valve with a small bellows. The valve coupling to the He cell is designed to minimize the contact surface to aluminum surfaces and silicon sealing O-rings (see Fig. 3). To open the valve, it is connected to a vacuum pump, and it is closed by atmospheric pressure. This upgrade reduced ^3He gas contamination (as observed from discharge spectra) and should also reduce polarization losses due to diffusion outside of the cell.

In the ^3He gas handling system, we employed all-metal bakeable valves, an oil free turbomolecular pump, and a residual gas analyzer (RGA). After extensive baking and pumping, the cryo-module is cooled down and the system is filled with about

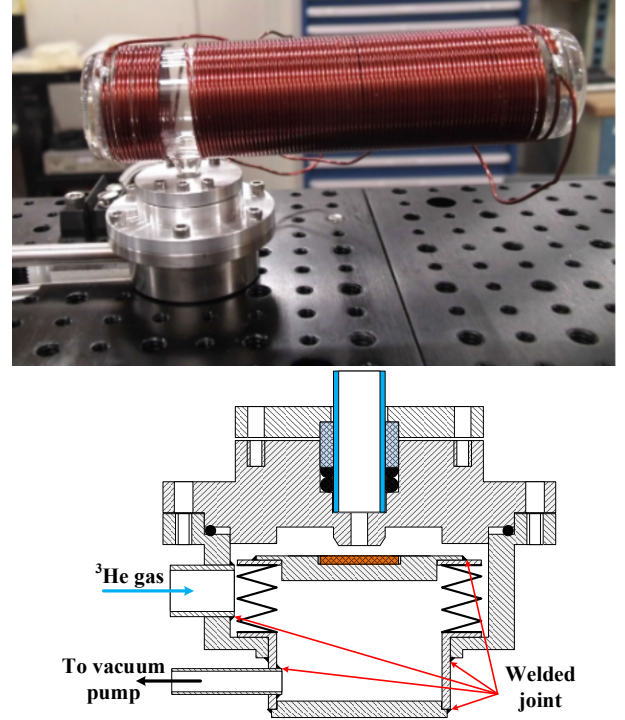


Figure 3: Top: “Open” ^3He gas cell (30 mm in diameter) with the isolation (filling) valve (IV) attached. Bottom: A new custom built pneumatic (bellows-based) isolation valve.

100 standard cm^3 of ^3He gas, which initially is absorbed by the cryo-pump and then released by heating the vessel to about 20 K to produce 3–5 Torr He gas pressure in the cell and gas supply manifold. The RF-discharge in the ^3He -cell is induced by inductive coupling with the 100 turns coil (see Fig. 3). This inductive coupling works better than capacitive coupling for the cell in the high magnetic field. The inductive coupling produces a more homogeneous plasma density distribution across the cell volume (in contrast to the capacitive coupling where the discharge is mostly induced near the cell walls). We use the master oscillator and a 60 dB broadband RF-amplifier to induce the discharge. The RF frequency is tuned for the best matching to the coil impedance. Typically, the RF-power is operated at about 44 MHz frequency. The He gas purity in the RF-induced discharge in the cell is monitored by the measurement of the relative brightness of the hydrogen Balmer-alpha line at 656 nm and adjacent ^3He spectral line at 668 nm. With the cryo-pumping, the hydrogen contamination from residual gas equilibrium pressure in the cryo-pump, or water dissociation by RF-discharge in the cell is the main contamination and it is well monitored by the optical spectrometer. It was experimentally established that for production of high ($> 80\%$) ^3He polarization, the relative hydrogen Balmer-alpha line brightness must be less than 2% of the He-line. After the extensive He-filling system pumping, baking and ^3He cryogenic purification, the hydrogen line was almost completely eliminated (see Fig. 4) and high ^3He polarization can be maintained for several (3–5) hours with the isolation valve closed (which is required for high polarization production). This is sufficiently long for the polar-

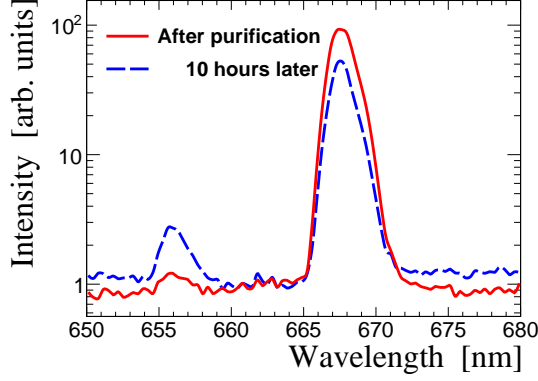


Figure 4: ^3He contamination monitoring. The hydrogen Balmer-alpha line intensity at 656 nm is strongly reduced, $< 0.4\%$ (red solid line), relative to the 668 nm ^3He line after the cryogenic purification cycle (cooling to 10 K) and increased to $\sim 3\%$ (dashed blue line) after 10 h of RF discharge with the isolation valve closed.

ized ^3He beam production in EBIS for the EIC fill.

We have studied a new EBIS drift-tube configuration to increase the gas efficiency (minimize amount of injected ^3He gas for the EBIS trap saturation). The ^3He gas was injected into the small (inner diameter 10–20 mm) drift tube by the pulsed valve. Estimates show that a very small amount of ^3He gas of about $(5\text{--}10) \times 10^{12}$ atoms will be required to be injected into the drift tube for $\sim 50\%$ EBIS trap neutralization. The total number of ^3He atoms in the 50 cm^3 at 3 Torr pressure is about 5×10^{18} atoms and only a small fraction will be used for the EIC fill. After a few hours cell operation with the closed isolation valve, some contamination is produced due to outgassing by discharge. There is plenty of time between injections to the EIC (typically ~ 8 h) to recirculate the ^3He gas in the system by turning the heater off, to pump gas in the cryopump to capture all the contamination and re-filling the cell to the operational pressure. This entire cycle takes about 10 min.

4. The ^3He Cell Layout Inside the 5.0 T EBIS Solenoid

A prototype layout for the optically-pumped ^3He cell inside the 5.0 T EBIS solenoid is presented in Fig. 5. The EBIS superconducting solenoid warm orifice diameter is 200 mm and we have to place the optically-pumped ^3He cell, injection valve and HV separation insulator in this radially very limited space. Fortunately, laser beams are transported in fibers and are quite compact.

We developed a pulsed valve for the ^3He -gas injection into the EBIS drift tube, which operates in the 5.0 T solenoid field. In this valve, the pulsed current of 10–20 A passes through the flexible springing plate (made of phosphor bronze with a thickness of 0.12 mm). The sealing Kalrez circular pad (5 mm in diameter, 1.0 mm thick) was attached to the plate. The induced Lorentz (Laplace) force: $\mathbf{F} = eL[\mathbf{I} \times \mathbf{B}] = 2\text{--}5\text{ N}$ (for $L=5\text{ cm}$ long plate) bends the plate and opens the small (0.1 mm in diameter) hole for the gas injection into the drift-tube. The valve prototype was tested in the 2.5 T solenoid field. A gas flow as low as 2×10^{12} atoms/pulse was measured at 12 A

current through the plate. The valve was also operated with the four consecutive pulses 4 ms apart, producing up to 10^{13} atoms/cycle. This might be an optimal mode for the gas injection distributed over 20 ms for the effective ionization by the EBIS electron beam, while limiting the injection gas cell pressure to $\sim 10^{-6}$ mbar.

The ^3He cell and gas preparation and filling system are at ground potential (actually at common HV EBIS potential of about 100 kV). The drift tube potential is about 20–30 kV. The ^3He cell and the pulsed injection valve are separated from the drift tube by a ceramic HV insulator. With the small amount of injected gas the pressure in the insulator is below 10^{-5} mbar. In addition, the high 5 T magnetic field reduces the ions transverse mobility which affects the discharge. We built a pulsed valve for the unpolarized gas injection into the EBIS using a two inches long ceramic insulator [see Fig. 6 (Top)]. It has been operated in the test EBIS setup by applying HV potential up to 40 kV.

5. ^3He Cell Optical Pumping and Polarization Measurements

For tests of ^3He optical pumping at high fields, the 30 mm “open-cell” was centered with the 152 mm warm-bore of a 3.0 T solenoid. To light the plasma discharge required to produce meta-stable states with the gas, a tightly-wound coil was driven with 44 MHz RF, which was 50% amplitude modulated at 297 Hz. The pumping laser was a Keopsys continuous-wave, Ytterbium-fiber laser, which could provide 10 W laser power at 1083 nm wavelength with a 2 GHz linewidth. This was tuned to pump the f_4^+ transition at 276.726 THz, and the laser frequencies were continuously monitored by WS-U wavemeter from HighFinesse.

The polarization was measured via the absorption of a second probe laser [15], a technique which we have used in previous studies to measure near 90% polarization with a 1 Torr sealed cell between 2.0 and 4.0 T [12]. A 70 mW distributed feedback laser from Toptica was used to allow the rapid tuning of the laser wavelength via changes to the diode temperature and current. The probe laser passed through the pumping cell and was reflected through the cell a second time, before arriving at a photodiode, which allowed the monitoring of the absorption of the light as a function of laser wavelength. Fig. 7 shows a measured ^3He absorption spectrum at 3.0 T, and includes the probe peaks used for these measurements at 276.76 THz. The ratio of the peak-heights of the transition pairs, $r = a_2/a_1$, allows the calculation of an absolute measure of the nuclear polarization when calibrated at zero polarization: $M = (r/r_0 - 1)(r/r_0 + 1)$ [15].

The amplitude modulation of the RF discharge at 297 Hz was used to improve the sensitivity of the measurement by passing the photodiode signal to a lock-in amplifier. This allowed the isolation of only the portion of the signal which came from interaction with the discharge, reducing noise from the photodiode and other light sources. The polarimeter DAQ was integrated into the common RHIC control system, and the software allowed the display of the spectrum as well as Gaussian fits to each probe peak to determine peak height while reducing the

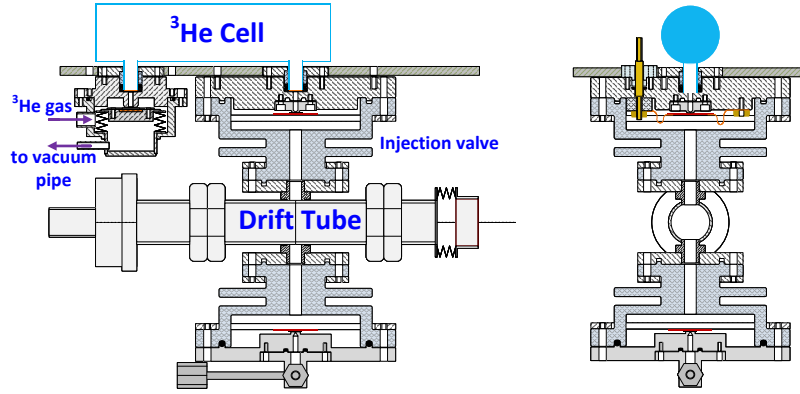


Figure 5: Optically-pumped ^3He cell layout inside of the 5 T EBIS solenoid. The warm bore diameter is 215 mm. Left: side view. Right: end view.



Figure 6: Top: the $[I \times B]$ pulsed ^3He injection valve with the moving springing plate and two current feedthroughs. Bottom: the injection valve for unpolarized gas injection, with the ceramic isolation section.

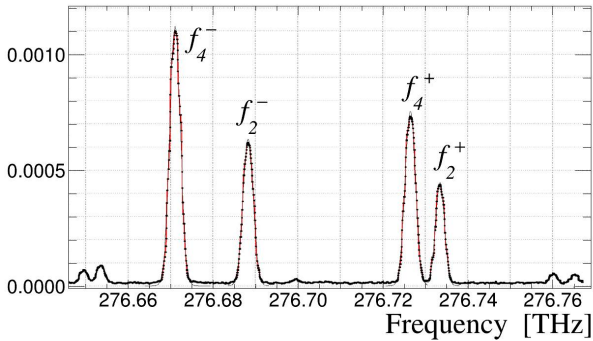


Figure 7: The ^3He absorption spectrum in a 2.0 T magnetic field. The f_{4-}^+ transition at 276.726 THz is used for optical pumping and a scan across transitions at 276.760 THz is used for the polarization measurements.

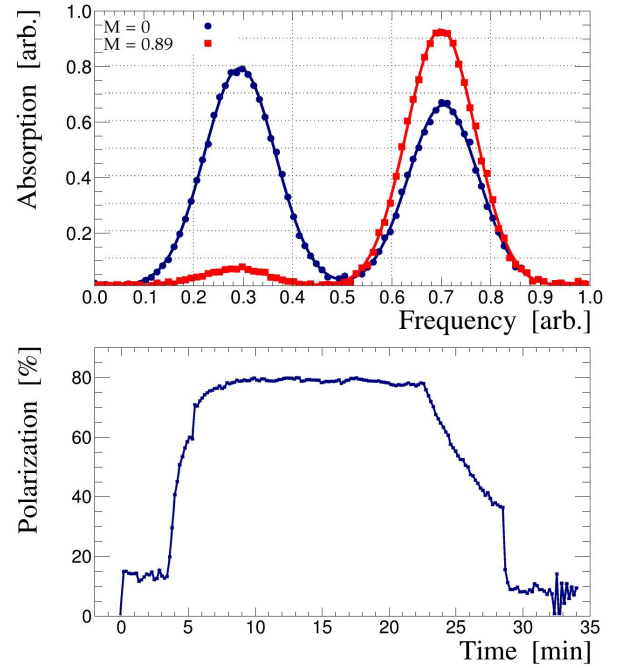


Figure 8: Top: example of the probe laser absorption signal for the 89% polarization in a sealed ^3He cell at 3.0 Torr pressure, compared with a signal at 0%. Bottom: polarization build-up vs. time. First 4 min the isolation valve is opened (13% polarization), after the valve was closed polarization increased to 80% in 5 min, at 22 min. the laser was switched off, and at 29 min. the isolation valve was opened.

effects of noise. An example of measurement is presented in Fig. 8.

The best results on optical pumping of ^3He gas in the “open” cell were $25 \pm 5\%$ with the open isolation valve and $80 \pm 5\%$ with the closed isolation valve at 3.0 Torr pressure. In these measurements we used a preliminary gas cryogenic purification system, with operational temperature $\sim 36\text{--}40\text{ K}$ (due to limited cooling power and higher heat transfer through the connecting tube). We also used a conventional brass Swagelock pneumatic isolation valve with the copper tube adapter to the ^3He cell. The gas purity has since been improved with the new cryogenic system and new isolation valve described above. We plan to

continue optical pumping studies with the new improved gas preparation system.

6. Chicane for Spin Rotation

Polarized ^3He ions extracted from EBIS will be accelerated by two linear accelerators to 2 MeV per nucleon. The spin direction will be parallel to the beam line and will need to be rotated to the vertical direction before the injection into the Booster synchrotron. The change of the spin direction will be done by the combination of a dipole and a solenoid. In the dipole field, the ion trajectory is deflected by $\theta = 21.5^\circ$. The dipole field also causes the spin to rotate with respect to the trajectory by 90° in the horizontal plane. Then the ion with the horizontally directed spin (perpendicular to the ion momentum) passes through the solenoid in which the spin is rotated around the solenoid axis by angle $\pm 90^\circ$ depending on the polarity of the solenoid field. Thus, the spin direction is changed to vertical, upward or downward. The deflected ion trajectory is returned to the straight beam line by the following three dipoles. The beam may optionally be steered straight to a polarimeter rather than returned to the Booster injection line. The overall beam line will form a trapezoidal chicane as shown in Fig. 9.

The beam optics design was done with TRACE 3-D [16] and confirmed by TraceWin [17]. The chicane was designed to be approximately symmetric to make it achromatic to minimize an emittance growth. The optics simulation showed that a 5 mA $^3\text{He}^{++}$ beam can be transported to the booster synchrotron and fit the transverse acceptance of the injection electrode with a required momentum spread ($\pm 0.5\%$).

A RF buncher is placed in front of the chicane to reduce the energy spread of the ions. The position was determined to have an appropriately long bunch width and a symmetric chicane. The effective voltage is 40 kV. The structure is a quarter-wave resonator with two gaps. The outer size is 335 mm \times 351 mm \times 580 mm. The bore is 80 mm in diameter and the gap length is 5 mm. The required RF power is 500 W.

The four identical dipoles are positioned at the vertices of the chicane. Two of them on the existing straight line are driven by a pulsed power supply to be turned on for ^3He ions and off for other ion species. The dipole shape is rectangular and the outer size is 536 mm (H) \times 364 mm (V) \times 538 mm (L). The pole width and the gap are 260 mm and 110 mm, respectively. The pole shim was designed to have a good field region within a diameter of 60 mm. The dipole is laminated for pulsed operation. The field is 0.19 T and the curvature of the trajectory is 1.6 m. 48-turns coils are wound around the upper and lower poles. The total current in each coil is 8.4 kA turn. The conductor has a 6.6 mm by 6.6 mm square cross-section with 4 mm diameter cooling channel. The inductance and the resistance will be 30 mH and 0.12 ohm. A trim coil is wound for the 2% field adjustment. The dipole was fabricated and the field was checked. The field strength was as designed. A significant difference of the field in ramp-up and ramp-down was not observed.

The solenoid will generate the integrated magnetic field strength of about 0.15 T-m for 90 degree spin rotation. The

field at the middle will be 0.66 T. The design is the same as used in the existing line. The inner diameter and the length of the coil are 145 mm and 202 mm, respectively. 1 kA will flow in a 9.5 mm \times 9.5 mm conductor with 6.3 mm cooling channel wound by 120 turns. The charge will be provided from a 9 mF capacitor bank. The charging time of the capacitor bank is about 0.2 s. The current waveform will be half-sine with the width of 12 ms. A bridge circuit with 4 Silicon Controlled Rectifiers (SCR) at the output will be used to reverse the current direction. 2 SCR on one pair of the diagonal lines will be on for one current direction while the other 2 SCR on the other pair will be on for the other current direction. The polarity of the solenoid can be changed for every pulse. The solenoid and the pulsed power supply were built. The field was generated as designed and it was confirmed that the power supply can work with 5 Hz at 1 kA peak.

To transport the beam, four quadrupoles and three steering magnets are installed. A Faraday cup at the end of the second dipole and a beam profile wire monitor between the second and the third dipoles will be used.

7. Absolute Nuclear Polarization Measurement at 6 MeV

To directly verify polarization of the fully stripped $^3\text{He}^{++}$ ions extracted from the EBIS, a spin asymmetry measurement in scattering from unpolarized ^4He gas will be carried out. In Ref. [18], it was shown that for spin-1/2 particles scattered from particles without spin, analyzing power $A_N(E_{\text{beam}}, \theta_{\text{CM}})$, as a function of the beam energy E_{beam} and the center-of-mass scattering angle θ_{CM} , must reach absolute maximum $|A_N| = 1$ at some point $(E_{\text{beam}}, \theta_{\text{CM}})$. To find the maximum, one can analyze experimentally determined phase shifts in the scattering. Using the experimental data [19], several such points were established [18, 20] for $^3\text{He}^4\text{He}$ elastic scattering including one (Fig. 10) in the energy range of the EBIS Linac. However, actual accuracy of the available experimental data does not allow to precisely predict the point location.

For 6 MeV polarized ^3He beam, the analyzing power has a local maximum, $A_N(6 \text{ MeV}, 96^\circ) > 0.9$, at $\theta_{\text{CM}} \approx 96^\circ$. By measuring the spin correlated asymmetry $a_N(T_h) = P_{\text{beam}} A_N(E_{\text{beam}}, \theta_{\text{CM}})$ as a function of the scattered ^3He kinetic energy T_h (kinematically, T_h is strictly correlated with θ_{CM}), one can determine the local maximum $a_N^{\text{max}}(E_{\text{beam}})$ (at some value of T_h^{max} or, equivalently, $\theta_{\text{CM}}^{\text{max}}$). Scanning the beam energy in the $5 < E_{\text{beam}} \leq 6 \text{ MeV}$ range, the absolute maximum $a_N^{\text{max}}(E_{\text{beam}}^{\text{max}}) = P_{\text{beam}}$ (at some beam energy $E_{\text{beam}}^{\text{max}} \approx 5.4 \text{ MeV}$) can be found. Consequently, we can calibrate analyzing power,

$$A_N(E_{\text{beam}} = 6 \text{ MeV}, T_h^{\text{max}}) = \frac{a_N^{\text{max}}(6 \text{ MeV})}{a_N^{\text{max}}(E_{\text{beam}}^{\text{max}})}, \quad (1)$$

for the 6 MeV beam energy. To implement the calibration method, the following should be considered:

- The ^3He beam polarization must be stable during the calibration. To verify the stability, multiple measurements with each E_{beam} can be used;

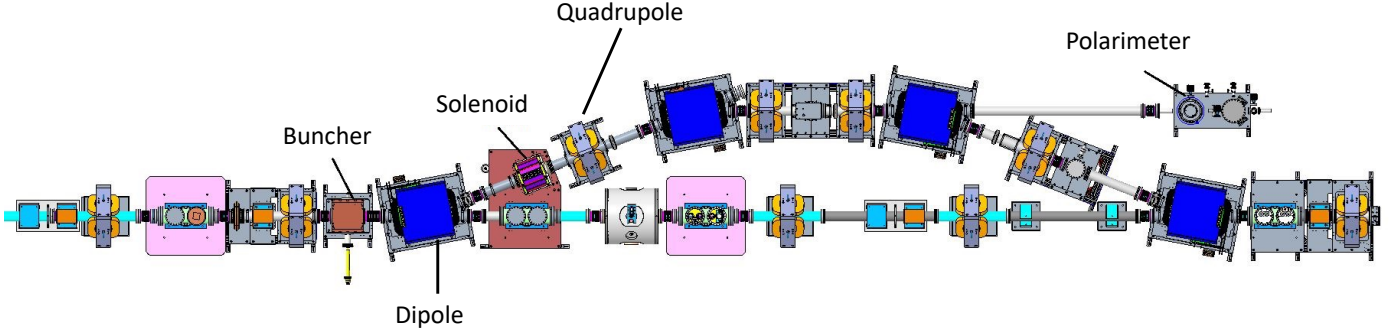


Figure 9: 3D drawing of the chicane for the spin rotation. The trapezoidal chicane will be attached to the existing straight line between the EBIS injector and the Booster synchrotron. The spin rotation will be accomplished by the first dipole and spin flip by the following solenoid.

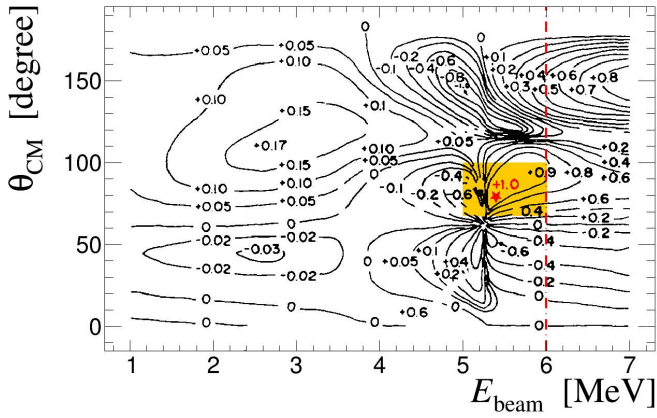


Figure 10: Polarization analyzing power in ${}^3\text{He}^4\text{He}$ elastic scattering versus the ${}^3\text{He}$ beam energy E_{beam} and the center-of-mass scattering angle θ_{CM} [20]. The expected location, $E_{\text{beam}} \approx 5.4$ MeV and $\theta_{\text{CM}} \approx 79^\circ$, of the absolute maximum $A_N = +1$ is shown by red star marker. The area proposed for experimental calibration of measured analyzing power at $E_{\text{beam}} = 6$ MeV (dashed red line) is shown by orange color.

- The scattered ${}^3\text{He}$ detector acceptance should be sufficiently large to isolate a local maximum of the asymmetry for any beam energy in the $5 < E_{\text{beam}} \leq 6$ MeV range;
- Two methods of variation of the ${}^3\text{He}$ beam energy are currently under consideration: (i) adjustment of the beam acceleration and (ii) changing the thickness of the polarimeter entrance window and, consequently, diluting the beam energy due to the dE/dx losses.

Also, it is important to note that for the ${}^3\text{He}$ beam energy $E_{\text{beam}} \leq 6$ MeV, there is no inelastic contributions to the ${}^3\text{He}^4\text{He}$ scattering.

8. The ${}^3\text{He}^4\text{He}$ Polarimeter Layout

The polarimeter layout is shown in Fig. 11. The polarized ${}^3\text{He}$ beam enters the scattering chamber through the thin aluminum foil window to minimize beam energy losses.

The scattering chamber is filled with 5 Torr ${}^4\text{He}$ gas. The effective target length of about ~ 1 cm is constrained by the collimators. Two Si detectors are located in the chamber at

$\theta_{\text{Lab}} = \pm 50^\circ$, 10 cm from the “center of the target”. The expected displacement ~ 0.2 mm of the scattered/recoil particles in the detector due to multiple scattering is small compared to the Si strip width.

The requirements on the detector geometry and measured energy range can be satisfied by Silicon strip detectors. For preliminary evaluation of the polarimeter performance we used the available Hamamatsu Si-photodiode array S4114-35Q [21]. Such a detector will cover center-of-mass angles $69^\circ < \theta_{\text{CM}} < 100^\circ$. The detected particles energy range is 2.6–4.2 MeV for ${}^3\text{He}$ and 1.5–3.4 MeV for ${}^4\text{He}$. The $30 \mu\text{m}$ depletion region is sufficient for stopping 5.5 MeV ${}^3\text{He}$ and 5.8 MeV ${}^4\text{He}$. The proposed design allows us to strongly suppress systematic errors. To this end, we can use many constraints resulting from the measured energy T , angle (the strip number) θ , and time-of-flight for both, scattered ${}^3\text{He}$ and recoil ${}^4\text{He}$. Detailed description of the ${}^3\text{He}^4\text{He}$ scattering kinematics in the measurements is considered in Ref. [22].

For energy calibration we will use ${}^{148}\text{Gd}$ (3.183 MeV) and ${}^{241}\text{Am}$ (5.486 MeV) α -sources. Both dead-layer and gain can be determined. This method was proven well in the RHIC polarimeters [23].

The expected energy resolution is $\sigma_E/E \leq 2\%$ and time resolution is $\sigma_t \leq 0.2$ ns. The Si strip structure (1 mm step) potentially provides a measurement of the scattering/recoil angle (lab. system) of about $\sigma_\theta \sim 0.2^\circ$. However, taking into account the effective size of the target (~ 1 cm), the effective angular resolution is about $\sigma_\theta \sim 1.2^\circ$, which corresponds to an effective $\sigma_E^{\text{geom}} \sim 0.1$ MeV.

The detector is equipped with a standard 12-channel preamplifier and shaper from the RHIC p-Carbon [24] and Hydrogen Jet Target polarimeter [25] (rise time ~ 20 ns and signal width ~ 60 ns). For Data Acquisition we plan to use the VME 250 MHz 14-bit waveform digitizers (SIS3316-250-14). Recording the full $20 \mu\text{s}/5000$ samples, the bunch signal in every readout channel is essential for monitoring the possible rate dependent systematic errors. The expected data rate in the polarization measurements is ~ 10 kB/sec per readout channel.

The preliminary evaluation of the polarimeter performance was based on the following assumptions about the ${}^3\text{He}$ beam: 6 MeV energy, 70% polarization, $5 \times 10^{11} \text{ s}^{-1}$ intensity, 1 Hz

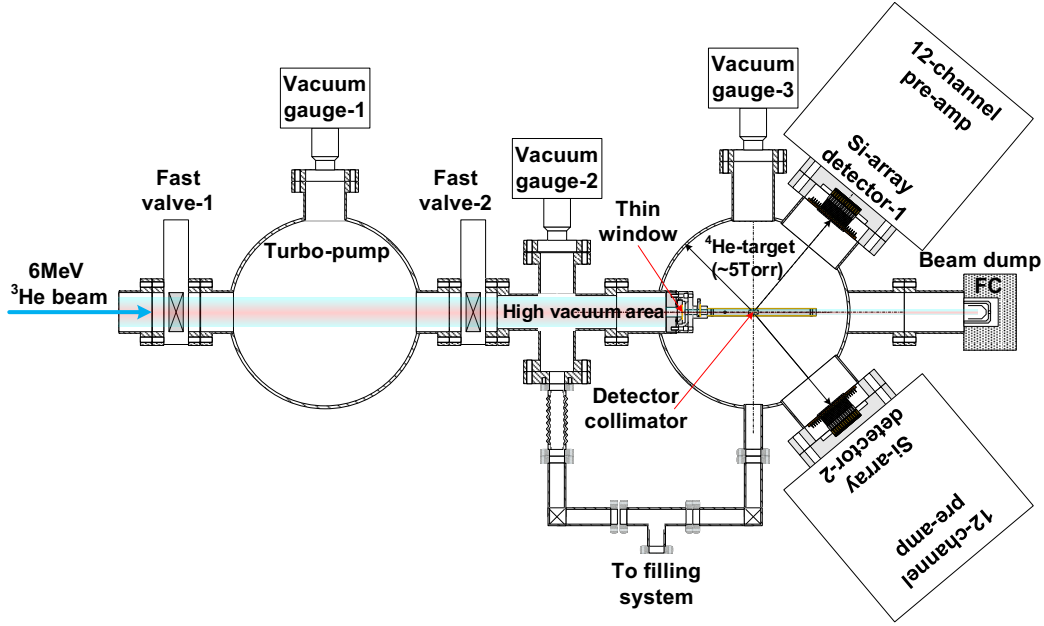


Figure 11: A layout of the $^3\text{He}^4\text{He}$ polarimeter. The effective target is a 1 cm long collimated part of the 5 Torr ^4He gas filled scattering chamber. The scattered ^3He and recoil ^4He angles, energies and time-of-flight are measured by the Si-strip detectors.

beam pulse repetition rate, and $\sim 20 \mu\text{s}$ pulse duration. For estimation, we also assumed $d\sigma/d\Omega \approx 50 \text{ mb/sr}$ cross section for the elastic $^3\text{He}^4\text{He}$ scattering at $E_{\text{beam}} = 6 \text{ MeV}$ and $\theta_{\text{CM}} = 90^\circ$.

For the effective 1 cm length of the target and 5 Torr gas pressure we will detect about 100 events per pulse (per second) in the center-of-mass scattering angle range of $69^\circ < \theta_{\text{CM}} < 100^\circ$. Thus, for t min of measurements, the statistical error in value of ^3He beam polarization is expected to be $(\delta P/P)_{\text{stat}} \lesssim 1.5\% \times (t/\text{min})^{-1/2}$. A preliminary estimate of the expected systematic error for the absolute ^3He beam polarization measurements (assuming detailed energy scan data are available) is $(\sigma_P/P)_{\text{syst}} \leq 1\%$.

9. Summary

The extended EBIS upgrade for heavy ion production was completed for the Run 2023. The next step will be integration of the ^3He polarizing apparatuses in the EBIS operation. The spin-rotator and the nuclear polarimeter (at 6 MeV beam energy) construction is in progress for completion by the end of 2023. The studies of the possible depolarization effects during polarized ^3He gas injection and multi-step ionization process in the EBIS, the optimization of the injection valve design, and the ^3He -cell geometry will be required to determine the maximum attainable polarization. The first EBIS operation for the polarized $^3\text{He}^{++}$ beam is planned in the Run 2024. The expected $^3\text{He}^{++}$ ion beam intensity is about 2×10^{11} ions/pulse and polarization $\geq 70\%$.

Acknowledgments

This research is funded by the DOE Research and Development Funds for the Next Generation Nuclear Physics Acceleration

tors Facilities.

References

- [1] I. Alekseev, A. C., M. Bai, et al., Polarized proton collider at RHIC, Nucl. Instrum. Meth. A **499** (2003) 392–414. [doi:10.1016/S0168-9002\(02\)01946-0](https://doi.org/10.1016/S0168-9002(02)01946-0).
- [2] Y. S. Derbenev, A. M. Kondratenko, S. I. Serednyakov, A. N. Skrinsky, G. M. Tumaikin, Y. M. Shatunov, Radiative Polarization: Obtaining, Control, Using, Part. Accel. **8** (1978) 115–126. URL <https://inspirehep.net/files/3d1ba4e45a59386e2b20da3d307b636a>
- [3] A. Accardi, L. Albacete, J., M. Anselmino, et al., Electron Ion Collider: The Next QCD Frontier, Eur. Phys. J. A **52** (9) (2016) 268. [arXiv:1212.1701](https://arxiv.org/abs/1212.1701), [doi:10.1140/epja/i2016-16268-9](https://doi.org/10.1140/epja/i2016-16268-9).
- [4] A. Zelenski, J. Alessi, Prospects On High-Intensity Optically-Pumped Polarized H^- , D^- , and $^3\text{He}^{++}$ Ion Source Development, Vol. 30 of ICFA Beam Dynamics Newsletter, 2003, pp. 39–42. URL https://icfa-usa.jlab.org/archive/newsletter/icfa_bd_nl_30.pdf
- [5] C. Epstein, R. Milner, Polarized ^3He Source Development at MIT, in: Opportunities for Polarized He-3 in RHIC and EIC, RIKEN BNL Research Center, September 28–30, 2011, Vol. 105, BNL-96418-2011-IR, 2011, pp. 25–30. URL <https://www.bnl.gov/isd/documents/76833.pdf>
- [6] C. S. Epstein, Development of a Polarized Helium-3 Ion Source for RHIC using the Electron Beam Ionization Source, Senior Thesis, Department of Physics, MIT (2013). URL <https://dspace.mit.edu/handle/1721.1/84388>
- [7] M. Abboud, A. Sinatra, X. Maître, G. Tastevin, P.-J. Nacher, High nuclear polarization of ^3He at low and high pressure by metastability exchange optical pumping at 1.5 Tesla, EPL **68** (2004) 480. [doi:10.1209/epl/12004-10237-y](https://doi.org/10.1209/epl/12004-10237-y).
- [8] K. Batz, S. Baeßler, W. Heil, E. W. Otten, M. Abboud, D. Rudersdorf, J. Schmiedeskamp, Y. Sobolev, M. Wolf, ^3He Spin Filter for Neutrons, J. Res. Natl. Inst. Stand. Technol. **110** (2005) 293–298. [doi:10.6028/jres.110.042](https://doi.org/10.6028/jres.110.042).
- [9] J. Maxwell, C. Epstein, R. Milner, J. Alessi, E. Beebe, A. Pikin, J. Ritter, A. Zelenski, Development of a Polarized Helium-3 Source for RHIC and eRHIC, Int. J. Mod. Phys. Conf. Ser. **40** (01) (2016) 1660102. [doi:10.1142/S2010194516601022](https://doi.org/10.1142/S2010194516601022).

- [10] A. Zelenski, G. Atoian, E. Beebe, D. Raparia, J. Ritter, J. Maxwell, R. Milner, M. Musgrave, Optically-pumped Polarized H^- and $^3He^{++}$ Ion Sources Development at RHIC, PoS **SPIN2018** (2018) 100. doi:[10.22323/1.346.0100](https://doi.org/10.22323/1.346.0100).
- [11] A. Zelenski, G. Atoian, E. Beebe, J. Maxwell, R. Milner, M. Musgrave, A. Poblaguev, D. Raparia, J. Ritter, Optically-pumped Polarized H^- and $^3He^{++}$ Ion Sources Development at RHIC, in: 9th International Particle Accelerator Conference (IPAC'18), Vancouver, BC, Canada, April 29 – May 4, 2018, JACoW Publishing, Geneva, Switzerland, 2018, pp. 644–646. doi:[10.18429/JACoW-IPAC2018-TUYGBE4](https://doi.org/10.18429/JACoW-IPAC2018-TUYGBE4).
- [12] J. D. Maxwell, J. Alessi, G. Atoian, E. Beebe, C. S. Epstein, R. G. Milner, M. Musgrave, A. Pikin, J. Ritter, A. Zelenski, Enhanced polarization of low pressure 3He through metastability exchange optical pumping at high field, Nucl. Instrum. Meth. A **959** (2020) 161892. arXiv:[1812.06139](https://arxiv.org/abs/1812.06139), doi:[10.1016/j.nima.2019.02.019](https://doi.org/10.1016/j.nima.2019.02.019).
- [13] J. G. Alessi, D. Barton, E. Beebe, et al., The Brookhaven National Laboratory electron beam ion source for RHIC, Rev. Sci. Instrum. **81** (2010) 02A509. doi:[10.1063/1.3292937](https://doi.org/10.1063/1.3292937).
- [14] A. Zelenski, G. Atoian, T. Lehn, D. Raparia, J. Ritter, High-intensity polarized and un-polarized sources and injector developments at BNL Linac, AIP Conf. Proc. **2373** (2021) 070003. doi:[10.1063/5.0057677](https://doi.org/10.1063/5.0057677).
- [15] K. Suchanek, M. Suchanek, A. Nikiel, T. Pałasz, M. Abboud, A. Sinatra, P.-J. Nacher, G. Tastevin, Z. Olejniczak, T. Dohnalik, Optical measurement of 3He nuclear polarization for metastable exchange optical pumping studies at high magnetic field, Eur. Phys. J. Special Topics **144** (2007) 67–74. doi:[10.1140/epjst/e2007-00109-8](https://doi.org/10.1140/epjst/e2007-00109-8).
- [16] K. R. Crandall, D. P. Rusthoi, Trace 3-D documentation: Second edition (12 1990).
- [17] D. Uriot, N. Pichoff, Status of TraceWin Code, in: 6th International Particle Accelerator Conference, 2015, p. MOPWA008. doi:[10.18429/JACoW-IPAC2015-MOPWA008](https://doi.org/10.18429/JACoW-IPAC2015-MOPWA008).
- [18] G. R. Plattner, A. D. Bacher, Absolute calibration of spin-1/2 polarization, Phys. Lett. B **36** (1971) 211–214. doi:[10.1016/0370-2693\(71\)90071-2](https://doi.org/10.1016/0370-2693(71)90071-2).
- [19] D. M. Hardy, R. J. Spiger, S. D. Baker, Y. S. Chen, T. A. Tombrello, Polarization in $^3He + ^4He$ elastic scattering, Phys. Lett. B **31** (1970) 355–357. doi:[10.1016/0370-2693\(70\)90193-0](https://doi.org/10.1016/0370-2693(70)90193-0).
- [20] W. R. Boykin, S. D. Baker, D. M. Hardy, Scattering of 3He and 4He from polarized 3He between 4 and 10 MeV, Nucl. Phys. A **195** (1972) 241–249. doi:[10.1016/0375-9474\(72\)90732-4](https://doi.org/10.1016/0375-9474(72)90732-4).
- [21] Hamamatsu S414-35Q, https://www.hamamatsu.com/resources/pdf/ssd/s4111-16r_etc_kmpd1002e.pdf.
- [22] G. Atoian, A. Zelenski, A. Poblaguev, Precision absolute polarimeter development for the $^3He^{++}$ ion beam at 5.0–6.0 MeV energy, PoS **PSTP2019** (2020) 045. doi:[10.22323/1.379.0045](https://doi.org/10.22323/1.379.0045).
- [23] A. A. Poblaguev, A. Zelenski, G. Atoian, Y. Makdisi, J. Ritter, Systematic error analysis in the absolute hydrogen gas jet polarimeter at RHIC, Nucl. Instrum. Meth. A **976** (2020) 164261. arXiv:[2006.08393](https://arxiv.org/abs/2006.08393), doi:[10.1016/j.nima.2020.164261](https://doi.org/10.1016/j.nima.2020.164261).
- [24] H. Huang, K. Kurita, Fiddling carbon strings with polarized proton beams, AIP Conf. Proc. **868** (2006) 3–21. doi:[10.1063/1.2401392](https://doi.org/10.1063/1.2401392).
- [25] A. Zelenski, A. Bravar, D. Graham, W. Haeberli, S. Kokhanovski, Y. Makdisi, G. Mahler, A. Nass, J. Ritter, T. Wise, V. Zubets, Absolute polarized H-jet polarimeter development, for RHIC, Nucl. Instrum. Meth. A **536** (2005) 248–254. doi:[10.1016/j.nima.2004.08.080](https://doi.org/10.1016/j.nima.2004.08.080).